

Beyond Target Networks: Improving Deep Q -learning with Functional Regularization

Alexandre Piché * [†]
Mila, Université de Montréal

Joseph Marino
California Institute of Technology

Gian Maria Marconi
RIKEN Center for Advanced Intelligence Project

Chris J. Pal
Canada CIFAR AI Chair, Mila,
Polytechnique Montréal,
Element AI – A ServiceNow Company

Mohammad Emtiyaz Khan
RIKEN Center for Advanced Intelligence Project

Abstract

Target networks are at the core of recent success in Reinforcement Learning. They stabilize the training by using old parameters to estimate the Q -values, but this also limits the propagation of newly-encountered rewards which could ultimately slow down the training. In this work, we propose an alternative training method based on functional regularization which does not have this deficiency. Unlike target networks, our method uses up-to-date parameters to estimate the target Q -values, thereby speeding up training while maintaining stability. Surprisingly, in some cases, we can show that target networks are a special, restricted type of functional regularizers. Using this approach, we show empirical improvements in sample efficiency and performance across a range of Atari and simulated robotics environments.

1 Introduction

Deep Q -learning (DQL) can be unstable when trained with both function-approximations and bootstrapping. These two comprise the two components of the so-called “deadly triad”, with the off-policy learning being the third one [1, 2]. The instability is largely due to the constantly changing target Q -values, e.g., due to the regular updating of the deep neural networks (DNNs) parameters, which are then constantly *chased* within a bootstrapping approach, overall yielding a regression problem of a non-stationary nature. Target networks improve stability by simply using a separate set of periodically updated parameters [3]. Due to its stability, target-network based training is now a standard practice in DQL [3, 4, 5, 6, 7, 8, 9] and has achieved state-of-the-art performance on a variety of difficult tasks, ranging from the Atari suite [10] to robotics applications [11].

Despite their impressive performance, using separate sets of parameters could be problematic. Since the parameters are not up-to-date, the target Q -values are lagging. When new rewards are encountered, it takes a while before they are *propagated* to the target Q -values. Multiple works have proposed alternatives to address this issue. A common approach has been to parameterize the target network using a moving average of the parameters [4], which is often not effective in practice. The approach

*Correspondence to alexandreliche@gmail.com

[†]Work done during an internship at RIKEN Center for Advanced Intelligence Project

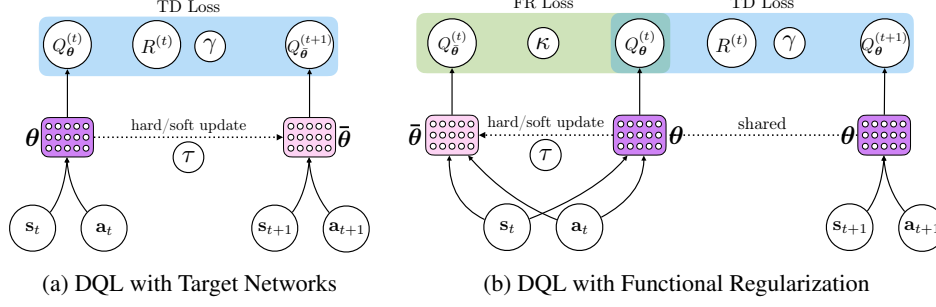


Figure 1: (a) Target networks use a separate set of parameters, $\bar{\theta}$ (pink) to estimate target values which is then used in the Temporal-Difference (TD) loss. This stabilizes the Q -value estimates, but is not up-to-date. (b) In our approach, we simply use the up-to-date θ to estimate the Q -value for the TD loss (see the rightmost block), and add a κ weighted Functional Regularization (FR) loss to stabilize the current Q -value estimate (parameterized by θ) by comparing it to the old Q -values (parameterized by $\bar{\theta}$).

can be seen as a simple *weight-regularization* method to slow down the parameter updates which might be insufficient for DNNs where regularizing the parameters does not necessarily imply stability of the network outputs [12]. Other alternatives based on preconditioning [13, 14] has also been proposed to maintain stability without the target networks. Such preconditioning uses a more sophisticated weight-regularization, e.g., based on Fisher information matrix, but is usually computationally costly and so far limited to simple network architectures.

In this paper, we go beyond target networks by using *functional regularization* (FR) to directly stabilize the DNN outputs [12, 15]. Instead of using a separate set of parameters for a target network which leads to lagging estimates, we simply use the up-to-date parameters to estimate the target (see Fig. 1). Our approach essentially “decouples” the two tasks of target estimation and stabilization. The decoupling enables us to explicitly tune the regularization level for a given task, which is not possible with target networks. In fact, we show that, in some cases, target networks themselves can be seen as a restrictive, special case of our FR approach. Through empirical investigations, we show that the proposed FR approach outperforms target networks across a range of tasks, such as Atari [16] and simulated robotics environments from OpenAI gym [17, 18]. Our approach is simple and can be implemented with only a few small changes in the existing codebases, but it improves the stability and speed of the overall DQL training.

2 Background

Preliminaries We consider the general case of a Markov Decision Process (MDP) defined by $\{\mathcal{S}, \mathcal{A}, P, R, \gamma, \mu\}$, where \mathcal{S} and \mathcal{A} respectively denote the finite state and action spaces, $P: \mathcal{S} \times \mathcal{A} \times \mathcal{S} \rightarrow \mathbb{R}$ are the environment transition dynamics, where $P(\cdot|s, a)$ is the distribution of the next state taking action a in state s . $R: \mathcal{S} \times \mathcal{A} \rightarrow \mathbb{R}$ denotes the reward function, $\gamma \in [0, 1)$ is the discount factor, and μ is the initial state distribution. We use an MDP to represent the sequential interaction between an agent and the environment, where at each round t the agent observes its current state s_t , selects an action a_t which results in a reward $R(s_t, a_t)$ and the next state $s_{t+1} \sim P(\cdot|s_t, a_t)$. The reinforcement learning (RL) objective involves defining an agent that maximizes the expected discounted sum of rewards $\mathbb{E}_{P, \pi} \sum_t \gamma^t R(s_t, a_t)$, (with $s_0 \sim \mu$), by means of a policy $\pi(a|s)$, that given a state selects in expectation the best action. Bellman optimality equations allow us to build such policy using the Q -value function, defined as:

$$Q^\pi(s, a) \equiv R(s, a) + \mathbb{E}_{P, \pi} \left[\sum_{t=1}^{\infty} \gamma^t R(s_t, a_t) \middle| s_0 = s, a_0 = a \right], \quad (1)$$

$$= R(s, a) + \gamma \mathbb{E}_{s', a' \sim P, \pi} [Q^\pi(s', a')], \quad (2)$$

Then, the optimal policy is $\pi^*(a|s) = \arg \max_a Q^{\hat{\pi}^*}(s, a)$. It can be estimated as $\hat{\pi}^*(a|s) = \delta(a - \arg \max_a Q^{\hat{\pi}^*}(s, a))$, where $\delta(\cdot)$ is the Dirac delta function, and we use $\hat{\pi}^*$ to evaluate the expectations in Eqs. (1) and (2) (see [19]).

Q-value Estimation We can estimate the Q -value for each state-action pair by formulating it as a regression problem, e.g., treating the right hand side of Eq. (1) as the target. However, because of the Monte Carlo expectation over the policy and environment dynamics, this will generally provide a high-variance target estimate [1]. Instead, we can minimize the one-step squared TD error for a given transition $(\mathbf{s}_t, \mathbf{a}, r_t, \mathbf{s}_{t+1}, \mathbf{a}_{t+1})$ [20]:

$$l^{\text{TD}}(\hat{Q}^\pi) = \frac{1}{2} \left(\underbrace{R(\mathbf{s}_t, \mathbf{a}_t) + \gamma \mathbb{E}_{\mathbf{s}_{t+1}, \mathbf{a}_{t+1} \sim P, \pi} [\hat{Q}^\pi(\mathbf{s}_{t+1}, \mathbf{a}_{t+1})]}_{\text{target } Q\text{-value}} - \hat{Q}^\pi(\mathbf{s}_t, \mathbf{a}_t) \right)^2. \quad (3)$$

This approach of using future value estimates as regression targets is referred to as *bootstrapping*.

Function Approximation In Eq. (3), \hat{Q}^π is estimated separately for each state-action pair, which is difficult in high-dimensional state-action spaces. Instead, we can approximate Q^π with a learned function, Q_θ (e.g., a deep network), with parameters θ [21, 22, 23]. Unfortunately, combining off-policy data, function approximation, and bootstrapping makes learning unstable and potentially diverge [1, 2, 14]. The problem arises when the parameters of the Q -network are updated to better approximate the Q -value of a state-action pair at the cost of worsening the approximation of other Q -values, including the ones used as targets.

One approach to stabilize learning involves estimating the regression targets with a *target network* $Q_{\bar{\theta}}$, where $\bar{\theta}$ are periodically updated [3]. Thus, the regression targets no longer directly depend on θ . With this, the TD loss for a given state transition is:

$$l^{\text{target}}(\theta) = \frac{1}{2} \left(R(\mathbf{s}_t, \mathbf{a}_t) + \gamma \mathbb{E}_{\mathbf{s}_{t+1}, \mathbf{a}_{t+1} \sim P, \pi} [Q_{\bar{\theta}}(\mathbf{s}_{t+1}, \mathbf{a}_{t+1})] - Q_\theta(\mathbf{s}_t, \mathbf{a}_t) \right)^2. \quad (4)$$

The target parameters can be updated after a fixed number of training iterations (“the hard update”) [3]. In between these updates, the target is using the old parameters, and the newly encountered rewards are not immediately reflected in the estimated target Q -values. The delay in the reward propagation could slow down the training. For instance, consider a Markov chain environment of N states with deterministic transitions, in which all states have reward of 0 except the terminal, right most state which has a reward of 1. Imagine using tabular Q -values and the corresponding target Q -values, which are updated every H training steps. Even with access to all the state-action pairs, this scheme will require NH training steps to propagate the right-most reward through the chain, i.e., to the state N steps away. While a table of target Q -values is not necessary in this case, it illustrates the point that using lagging target-values slows down the training.

An alternative to hard-updating is to use a moving average of the weights to parametrize the target Q -network as done with Polyak’s averaging (“the soft update”) [4]. The target network’s weights are updated as $\bar{\theta} \leftarrow (1 - \tau)\bar{\theta} + \tau\theta$, where $\tau \in (0, 1)$ is the update rate. However, we are not using θ to estimate the target Q -values. Thus, our regression targets are no longer up-to-date and learning is slowed.

Weight Regularization in DQN The soft updates can be seen as a simple *weight regularization* where the update of $\bar{\theta} \leftarrow \theta$ is delayed by adding an L_2 regularizer $\tau\|\theta - \bar{\theta}\|^2$. Essentially, we do not want the value of $\bar{\theta}$ to abruptly change. Such weight-regularization to improve stability is common in non-stationary time-series analysis [24, 25, 26], online learning [27], and continual learning [28, 29] in general. Recent attempts to go beyond target networks employ preconditioning methods which can also be seen as weight-regularization methods [13, 14]. For example, natural-gradient descent used in [13] employs the Kullback-Leibler (KL) for Gaussian distributions $\mathcal{N}(q|Q_\theta(s, a), 1)$ over the Q -values q , giving rise to a quadratic weight-regularizer. Another approach of [14] uses a different preconditioner which can also be seen as a quadratic weight-regularization. The computation in these approaches is challenging and so far they have only been applied to small networks.

A more serious problem with weight regularization is its ineffectiveness for DNNs. For neural networks, the network outputs depend on the weights in a complex way and exact value of the weights may not matter much. What matters ultimately is the network outputs [12], and it is better to directly regularize those. Recently such *functional regularization* has been applied to continual learning [15] to avoid catastrophic forgetting, where it has shown to perform much better than weight-regularization.

We will resort to this approach in this paper to improve the stability of DQL without using target networks.

3 Deep Q -learning with Functional Regularization

Target networks stabilize the non-stationarity that arises when combining function approximation and bootstrapping. However, by not using the most up-to-date target Q -value estimates, this also has the effect of slowing down training. Intuitively, since the lagging network is used to estimate the target Q -value, it can be interpreted as a form of *prior*, preventing the Q -value estimates from changing too quickly. In this section, we use this insight to introduce FR Q -learning, a regularized loss to stabilize training while using up-to-date target values. In the process, we help formalize the notion of target networks as a form of functional prior.

3.1 Functional Regularization

We can see target networks as having a dual role: providing target Q -values used for learning, and stabilizing training. We can separate these two roles: use up-to-date parameters to estimate the target Q -values, and use a functional prior to regularize the Q -values. Following [12], we propose to use an L_2 functional regularizer which penalizes the divergence between the current Q -value function $Q_\theta(\mathbf{s}, \mathbf{a})$ and old $Q_\theta(\mathbf{s}, \mathbf{a})$. This gives us the following loss function where up-to-date parameter θ are used in the TD loss along with a FR loss to stabilize θ by regularizing the current state-action pair only,

$$l^{\text{FR}}(\theta) = \frac{1}{2} \left(R(\mathbf{s}_t, \mathbf{a}_t) + \text{stop_grad}(\gamma \mathbb{E}[Q_\theta(\mathbf{s}_{t+1}, \mathbf{a}_{t+1})]) - Q_\theta(\mathbf{s}_t, \mathbf{a}_t) \right)^2 + \frac{\kappa}{2} \left(Q_\theta(\mathbf{s}_t, \mathbf{a}_t) - Q_{\bar{\theta}}(\mathbf{s}_t, \mathbf{a}_t) \right)^2. \quad (5)$$

The expectation above is taken over the transition and policy, and $\kappa > 0$ is the regularization parameter. By `stop_grad`, we indicate a function that prevents gradients from propagating into the target Q -value estimate.

Critically, unlike Eq. (4), the target Q -value estimates are supplied by the up-to-date Q -network, with the functional prior now separately serving to stabilize the estimate. As with a target network, we can update the functional prior periodically. Overall, l^{FR} is arguably similar in complexity to l^{target} , requiring only an additional function evaluation for $Q_\theta(\mathbf{s}_{t+1}, \mathbf{a}_{t+1})$ and an additional hyperparameter, κ , which we found was not difficult to tune in our experiments (see Section 4). As will be discussed in Section 3.2, target networks implicitly make a fixed trade-off between speed and stability, whereas κ provides needed flexibility in adjusting this trade-off.

Functional regularization of the Q -network outputs has multiple advantages over regularization of the Q -network parameters [13, 14, 30]. DNN parameter regularization is difficult to interpret and tune, as the effect of parameters may vary substantially within and across architectures. While various architectures can be used to parameterize Q -networks, the interpretation of the output Q -value is consistent in all settings. FR provides a straightforward way to decouple target value estimation and stability (via regularization). FR is also compatible with ensembles of Q -networks [7, 9, 31, 32].

Similarly to [13], this can also be seen as a KL divergence between two Gaussian process whose mean function is simply the Q -values at different state-action pairs and covariance function is simply the identity. It is indeed possible to inject correlations, and also regularize multiple past state-action pairs. Since this increase the computation cost, we did not pursue this in this work.

3.2 Interpreting Target Networks through Functional Regularization

Given that FR also stabilizes estimation through the use of a lagging estimate, we might reasonably ask whether target networks can be interpreted through the lens of FR. To approach this question, we compare the gradients, $\nabla_\theta l(\theta)$, arising from each case (Eq. (4) & Eq. (5)) allowing us to see how these learning procedures differ. For a complete derivation, see Appendix A.2. To simplify notation, we define the Q -value estimate at time t as $Q_\theta^{(t)} \equiv Q_\theta(\mathbf{s}_t, \mathbf{a}_t)$, the corresponding expected change

in the Q -value estimate as $\Delta Q_\theta^{(t)} \equiv \mathbb{E}_{P,\pi}[Q_\theta^{(t+1)} | \mathbf{s}_t, \mathbf{a}_t] - Q_\theta^{(t)}$, and the reward as $R^{(t)} \equiv R(\mathbf{s}_t, \mathbf{a}_t)$. Then, for a given state-action pair, we can compare the two gradients:

$$\nabla_\theta l^{\text{FR}}(\theta) = -(R^{(t)} + \gamma(Q_\theta^{(t)} + \Delta Q_\theta^{(t)}) - Q_\theta^{(t)}) \nabla_\theta Q_\theta^{(t)} + \kappa(Q_{\bar{\theta}}^{(t)} - Q_\theta^{(t)}) \nabla_\theta Q_\theta^{(t)}. \quad (6)$$

Replacing $\Delta Q_\theta^{(t)}$ with $\Delta Q_{\bar{\theta}}^{(t)}$ and κ with γ we recover the gradient of $l^{\text{target}}(\theta)$:

$$\nabla_\theta l^{\text{target}}(\theta) = -(R^{(t)} + \gamma(Q_\theta^{(t)} + \Delta Q_{\bar{\theta}}^{(t)}) - Q_\theta^{(t)}) \nabla_\theta Q_\theta^{(t)} + \gamma(Q_{\bar{\theta}}^{(t)} - Q_\theta^{(t)}) \nabla_\theta Q_\theta^{(t)}. \quad (7)$$

We see that, despite differences in their loss formulations, target networks and FR result in nearly identical gradients, with two key exceptions. The first distinction, underlined in orange, is the estimated change in the Q -value. With target networks, this term is supplied by the lagging network parameters, $\bar{\theta}$, and therefore is not up-to-date, whereas with FR, it is supplied by the up-to-date parameters. Thus, FR can more quickly propagate updated value estimates. The second distinction, underlined in blue, is the weighting on the difference between the lagging and up-to-date Q -value estimates. With target networks, this is the discount factor, γ , whereas with FR, this is a separate hyper-parameter. Using the gradient in Eq. (7), and defining $\hat{Q}_{\theta, \bar{\theta}}^{(t)} \equiv Q_\theta^{(t)} + \Delta Q_{\bar{\theta}}^{(t)}$, we can derive a loss function, $\tilde{l}^{\text{target}}$, that yields equivalent gradients as l^{target} , but is written in the FR form:

$$\begin{aligned} \tilde{l}^{\text{target}}(\theta) = \frac{1}{2} \left(R(\mathbf{s}_t, \mathbf{a}_t) + \text{stop_grad} \left(\gamma \mathbb{E} \left[\hat{Q}_{\theta, \bar{\theta}}(\mathbf{s}_{t+1}, \mathbf{a}_{t+1}) \right] \right) - Q_\theta(\mathbf{s}_t, \mathbf{a}_t) \right)^2 + \\ \frac{\gamma}{2} \left(Q_\theta(\mathbf{s}_t, \mathbf{a}_t) - Q_{\bar{\theta}}(\mathbf{s}_t, \mathbf{a}_t) \right)^2. \end{aligned}$$

From this perspective, target networks effectively perform a special, restricted form of Gaussian FR, with $p(Q_\theta) = \mathcal{N}(Q_{\bar{\theta}}, \gamma^{-1})$, i.e., a precision weight that is not under direct control. In contrast, l^{FR} allows us to separately adjust this weight to trade-off stability and learning speed. Overall, this analysis frames target networks as closely related to FR, but with lagging target value estimates and an inability to separately control the regularization weight.

3.3 Comparison with Polyak averaging

We mentioned Polyak's averaging as an alternative to hard updates. Interestingly, if we assume the target network is an estimate in weight space of the latest Q -network, we can show that Polyak's updates implicitly operate parameter regularization on such estimate. Suppose that after each gradient step (indexed by i) we identify the target network as the solution to the problem:

$$\bar{\theta}_{i+1} = \min_{\bar{\theta}} \frac{1}{2} \|\bar{\theta} - \theta_i\|^2 + \frac{1-\tau}{2\tau} \|\bar{\theta} - \bar{\theta}_i\|^2 \quad (8)$$

where θ_i is the latest set of weights of the Q -network and $\bar{\theta}_i$ is the previous instance of the target network. The minimizing $\bar{\theta}$ is obtained by computing the gradient of the problem and equating it 0. This leads to $\bar{\theta}_{i+1} = (1-\tau)\theta_i + \tau\bar{\theta}_i$, which is exactly Polyak's averaging. This shows that Polyak's update is indeed a form of weight regularization with respect to the most recent target network. However, weight regularization does not guarantee that the output of the regularized network matches the previous target network. In fact, while this technique has found success in control problems [4, 6, 7], hard updating of the parameters is usually preferred for complex DNN architectures [8, 10, 33, 34].

3.4 Convergence of FR Q -learning in the Tabular Setting

Having introduced and explained FR Q -learning, we now provide a theoretical convergence result in the tabular setting, guaranteeing that the introduction of functional regularization does not prevent convergence.

Theorem 1. *Given a tabular Q -function $Q_t : \mathcal{S} \times \mathcal{A} \rightarrow \mathbb{R}$, consider the iteration*

$$\begin{aligned} Q_{i+1}(\mathbf{s}_t, \mathbf{a}_t) = Q_i(\mathbf{s}_t, \mathbf{a}_t) + \rho_i(\mathbf{s}_t, \mathbf{a}_t) \{ R(\mathbf{s}_t, \mathbf{a}_t) + \gamma \tilde{Q}_i - Q_i(\mathbf{s}_t, \mathbf{a}_t) \} + \\ + \kappa_i(\mathbf{s}_t, \mathbf{a}_t) (Q_i(\mathbf{s}_t, \mathbf{a}_t) - \bar{Q}_i(\mathbf{s}_t, \mathbf{a}_t)) \end{aligned}$$

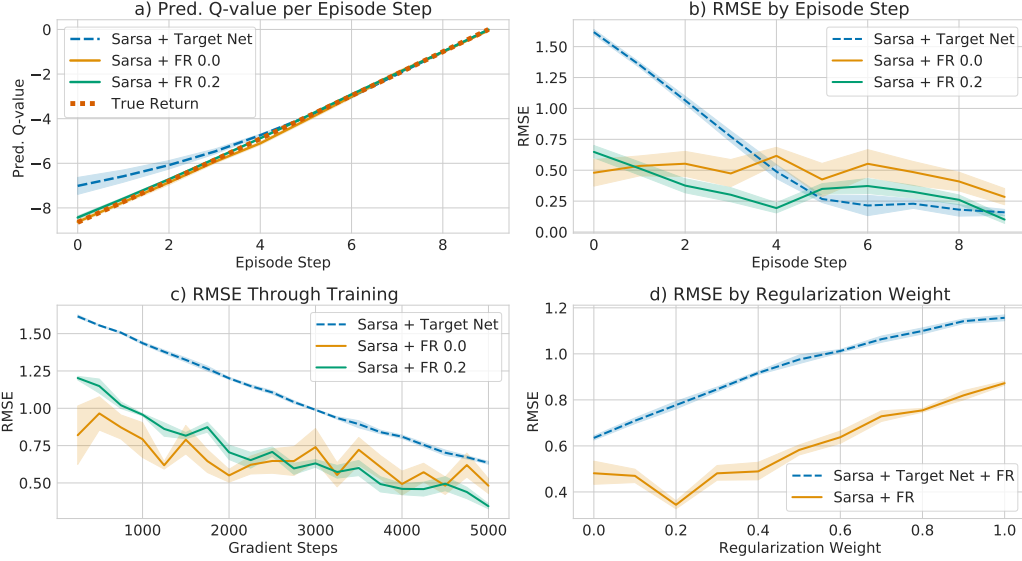


Figure 2: **Policy Evaluation Analysis.** We compare FR Sarsa (on-policy Q -learning) against Sarsa with and without target networks on FetchPush-v1. Target networks result in slower learning, whereas not using target networks (FR 0.0) results in more instabilities. FR maintains stability while improving learning speed, with the FR weight, κ , determining this trade-off.

where $\tilde{Q}_i = Q_i(\mathbf{s}_{t+1}, \mathbf{a}_{t+1})$ with $\mathbf{s}_{t+1} \sim P(\mathbf{s}|\mathbf{s}_t, \mathbf{a}_t)$ and $\mathbf{a}_t \sim \pi^*(\mathbf{a}|\mathbf{s}_t)$.

Consider the following assumptions: $\tilde{Q}_i = Q_{i-I}$ for some positive integer I (that can change between iterations); $\rho_i(\mathbf{s}_t, \mathbf{a}_t)$ is a positive sequence such that $\sum_{i=0}^{\infty} \rho_i(\mathbf{s}_t, \mathbf{a}_t) = \infty$, $\sum_{i=0}^{\infty} \rho_i^2(\mathbf{s}_t, \mathbf{a}_t) < \infty$, $\forall \mathbf{s}, \mathbf{a}$; $\kappa_i(\mathbf{s}_t, \mathbf{a}_t)$ is a sequence such that $\lim_{i \rightarrow \infty} \kappa_i(\mathbf{s}_t, \mathbf{a}_t) / \rho_i(\mathbf{s}_t, \mathbf{a}_t) \rightarrow 0$ and $\kappa_i(\mathbf{s}, \mathbf{a}) \leq 1/2 \quad \forall \mathbf{s}, \mathbf{a}$; every state is visited infinitely many times with probability 1. Then, the iteration converges to the minimum of Eq. (3) with probability 1.

The proof is provided in Appendix A.5. This implies that solving Eq. (5) with stochastic gradient descent converges to the optimal Q -function with probability 1. We make a remark on the regularization coefficient κ . The proof relies on a sequence $\kappa_i(\mathbf{s}_t, \mathbf{a}_t)$ that converges to 0, while, in our experiments, we use a constant κ across i and t . However, it can be shown that if the difference between the current estimates of the Q -values and the lagging estimates becomes asymptotically smaller fast enough, then $\kappa_i(\mathbf{s}_t, \mathbf{a}_t)$ can be constant. Indeed, our experiments suggest that functional regularization accelerates the convergence, therefore $(Q_i(\mathbf{s}_t, \mathbf{a}_t) - \tilde{Q}_i(\mathbf{s}_t, \mathbf{a}_t))$ is expected to become small fast enough, allowing for κ to be fixed.

4 Experiments

Target networks are utilized for value estimation in both discrete [3] and continuous [4] action spaces, often using hard and soft parameter updates, respectively. Thus, to demonstrate the benefits of FR Q -learning over target networks, we perform experiments in both settings. Specifically, we compare performance on the same subset of Atari games [16] used by Mnih et al. [3], as well as the suite of multi-goal continuous control tasks [18, 35] from OpenAI gym [17]. In all cases, the experimental setup is identical across FR and the baseline target network approach, the only difference being the use of l^{FR} (Eq. (5)) instead of l^{target} (Eq. (4)).

4.1 Q -Value Estimation with a Fixed Policy

Functional regularization provides a technique for improving the learning speed of Q -value estimation while maintaining stability. This, in turn, improves the agent’s policy, enabling faster overall task learning. To tease apart this interaction and demonstrate the impact of FR, we isolate value estimation from policy optimization. We compare different policy evaluation algorithms on FetchPush-v1

from the multi-goal suite using trajectories collected by a fixed expert policy. The task consists of pushing a block to a designated goal area, with a reward of 0 if the goal has been reached and -1 otherwise. Thus, the true discounted return is the negative discounted number of steps required to complete the task. By comparing the estimated Q -values with the true discounted return, we can evaluate the learning speed and stability of various approaches.

Given that we are estimating values for a fixed policy, we use Sarsa [36], an on-policy TD-learning approach, estimating the expectation within the target values (see Eq. (3)) using an action sampled from the fixed policy. We compare three variants of Sarsa, each corresponding to a different value loss: **1)** l^{target} with Polyak updating (“Sarsa + Target Net”), **2)** no target network, i.e., estimating target Q -values with the most up-to-date parameters and no regularization (“Sarsa + FR 0.0”), and **3)** l^{FR} with $\kappa = 0.2$ (“Sarsa + FR 0.2”). These comparisons allow us to assess how target networks and FR affect stability and learning speed.

In **Fig. 2a**, we plot the estimated Q -values for the first 10 time steps of an episode (until the agent reaches the goal) after 5,000 gradient updates, along with the true discounted return. As compared with FR, using a target network results in slower reward propagation, still incorrectly estimating the Q -values over the first 3 steps. To examine this more closely, we plot the Root Mean Squared Error (RMSE) from the true return in **Fig. 2b**, where we see that FR with $\kappa = 0.2$ is more accurate than not using a target network (FR 0.0), maintaining relatively accurate Q -values throughout. To see how this varies during training, in **Fig. 2c**, we plot the RMSE, averaged over time steps within an episode, throughout the first 5,000 gradient updates. While target networks result in stable training, they significantly slow down learning speed. Without a target network (FR 0.0), learning speed is improved at the cost of reduced stability. FR obtains the best of both setups, with fast, yet relatively stable training. Finally, in **Fig. 2d**, we plot the RMSE after 5,000 gradient updates for FR with $\kappa \in [0.0, 1.0]$. Performance varies fairly smoothly as a function of regularization weight, obtaining the optimum at the intermediate value of $\kappa = 0.2$. For completeness, we also plot the RMSE when using both a target network and FR (“Sarsa + Target Net + FR”). This over-regularizes training, resulting in worse accuracy.

Eventually, after a large number of gradient updates, we would expect target networks and FR to both converge, approximating the true Q -value. In practice, however, a small number of gradient updates are performed (typically just a single update [4]) before the Q -network is used to improve the policy. Thus, short-term learning speed and stability, as analyzed in Fig. 2, become even more important when also optimizing the policy. In the following sections, we analyze this setting, where we observe that the shortcomings of target networks (and lack thereof) are amplified. That is, target networks consistently result in slower learning speed, whereas not using target networks or any other form of regularization results in instabilities, thereby harming performance. FR, in contrast, can trade-off between these two extremes, yielding shorter-term improvements in learning speed with longer-term improvements in stability (Fig. 2c).

4.2 Atari

The Arcade Learning Environment [16] provides a set of benchmark Atari games for evaluating RL algorithms, with rich visual observations and diverse reward functions. Due to the complexity of these environments, complex DNN architectures are preferred and hard value network updates are typically used. To evaluate FR in this setting, we compare with a vanilla Deep Q -network (DQN) [3], allowing us to isolate the benefits of FR. We use the same set of hyperparameters as used in the baseline from Hessel, et al. [10], which can be found in Table 2 in the Appendix. For experiments, we use the same suite of representative environments from Mnih et al. [3], with results averaged over 5 random seeds.

Atari performance results are presented in Fig. 3, comparing the baseline DQN against FR with various regularization weights, $\kappa \in \{0.0, 0.5, 0.75, 1.0\}$. Across all environments, FR matches or exceeds DQN in terms of sample efficiency and final performance at 10M steps. Each seed takes 1 week to run on our resources for a total of 175 weeks of gpu usage. Without any form of regularization (FR $\kappa = 0.0$), i.e., DQN without a target network, performance is generally poor, typically failing to learn at all due to non-stationarity. With FR, reducing κ tends to improve sample efficiency, as the effects of regularization are diminished. However, even with $\kappa = 1.0$, we see that FR generally outperforms DQN, which has an effective regularization weight of $\kappa = \gamma = 0.99$

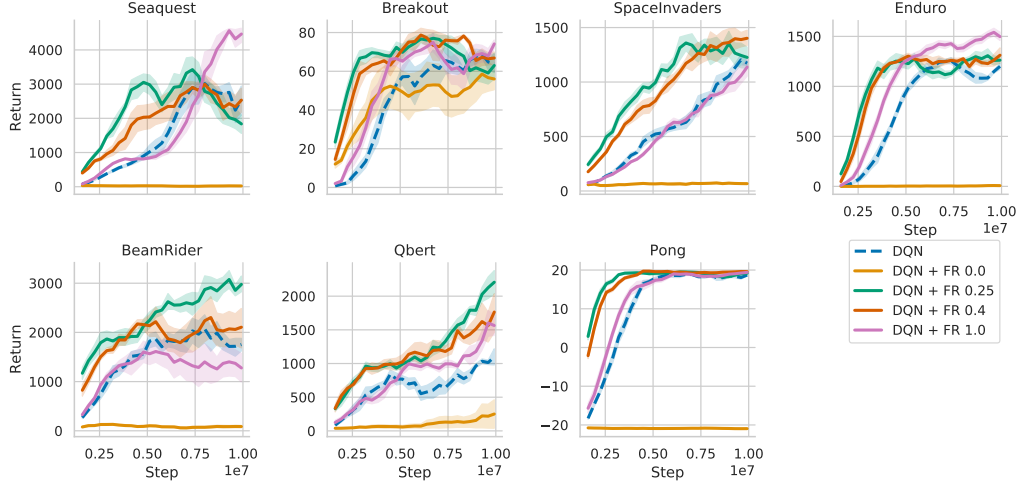


Figure 3: **Atari Performance.** Performance curves for the subset of Atari games from Mnih et al. [3]. The baseline (dotted blue line) and 4 different FR weights (solid lines) average returns over 5 trials using ϵ -greedy with $\epsilon = 0.05$.

(see Section 3.2). Thus, FR’s ability to use up-to-date target Q -values also plays a significant role in improving performance over target networks. We present additional Atari results in Appendix A.4.2.

4.3 Multi-Goal Environments

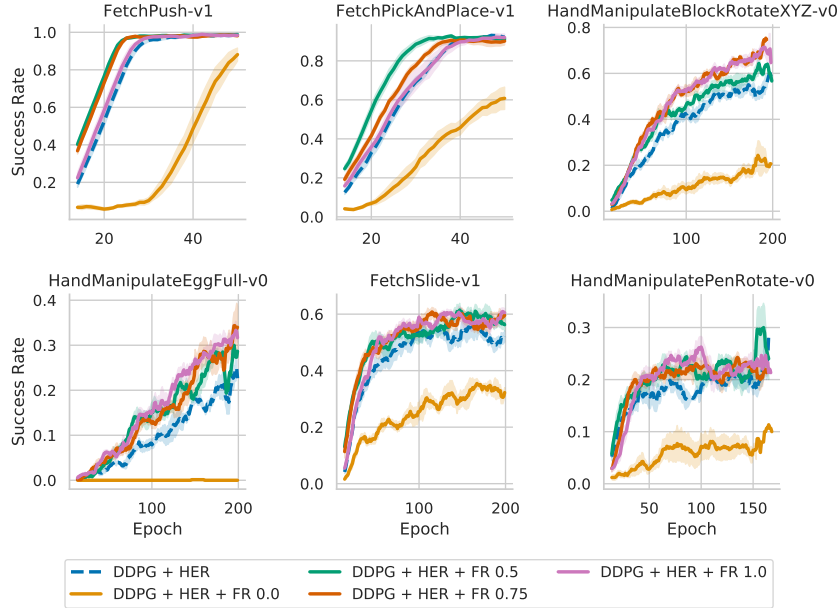


Figure 4: **Multi-Goal Environment Performance.** Performance curves for a subset of sparse-reward robotic tasks. Results for the baseline (dotted blue line) and multiple FR weights (solid lines) are reported by averaging success rates over 10 trials under the greedy policy.

The multi-goal environments from OpenAI gym [17, 18, 35] are of a suite of sparse-reward robotic tasks implemented using the MuJoCo physics engine [37]. As noted by Plappert et al. [18], current RL algorithms, such as Deep Deterministic Policy Gradient (DDPG) [4], struggle to solve these tasks due to their sparse, binary rewards. To address this issue, Hindsight Experience Replay (HER)

[38] re-labels transitions such that rewards are encountered more frequently during training. The combination of DDPG + HER, using soft value network updating, performs well on the multi-goal environments, and we therefore use it as a baseline in evaluating FR. Further, by using HER as the exploration strategy in both cases, we can isolate the effects of improved reward propagation in FR. We use the same set of hyperparameters as Plappert et al. [18], which can be found in Table 1 in the Appendix.

We present results on the multi-goal environments in Fig. 4, again evaluating FR with various values of $\kappa \in \{0.0, 0.5, 0.75, 1.0\}$. Results are reported using 5 random seeds for each setting, with success rates evaluated using 10 trials under the greedy policy. Each seed takes at most 3 days to run for the most intensive tasks which is roughly equivalent to 450 days of gpu usage.. FR matches or outperforms the baseline DDPG + HER across all environments, both in sample efficiency and final performance at 200 epochs. As with Atari, a lack of regularization (FR $\kappa = 0.0$), i.e., DDPG + HER with no target network, performs poorly, particularly on more challenging environments. On the simpler environments, FetchPush-v1 and FetchPickAndPlace-v1, smaller values of κ yield improvements in sample efficiency. However, the results are more similar on the more challenging environments. FR with $\kappa = 1.0$ outperforms the baseline (with an effective $\kappa = \gamma = 0.98$), providing further evidence that using up-to-date target values is a significant benefit of FR. Additional Mujoco experiments are provided in the Appendix A.4.1, but FR does not provide significant improvements as the reward is dense and the DNN architectures are simple.

5 Related Work

Multiple previous works have investigated improving value estimation through various constraints and regularization. Farahmand et al. [39] is perhaps the closest work to our own, functionally regularizing the L_2 norm of the Q -value estimate, i.e., penalizing $\kappa \|Q_\theta\|^2$. This can be interpreted as using a fixed Gaussian prior, whereas we use a periodically updated set of parameters to provide a moving prior. Other works have sought to regularize the Q -value estimator by constraining parameter updates, e.g., through conjugate gradient methods [40], pre-conditioning the gradient updates [13, 14], or using Kalman filtering [30, 41]. As argued in Sections 2 and 3, functional regularization, as opposed to parameter regularization, is more appropriate in this setting, as parameter regularization does not necessarily imply that the Q -value estimates remain stable during training. Additional works have regularized the Q -value estimator using temporal regularization [42, 43, 44], smoothing value estimates over trajectories. In contrast, FR Q -learning regularizes value estimates across training updates to maintain stability. Other works have proposed methods for regularizing policy optimization using trust regions [45, 46], proximal methods [47], entropy/KL penalties [5, 6, 48], and natural policy gradients [49]. As these methods are applied to a separately parameterized policy, they can readily be combined with FR Q -learning. Finally, while we apply FR to improve value estimation in RL, FR has also been used in a variety of other settings, such as supervised learning [12, 50], unsupervised learning [51], and continual learning [15]. Similarly, works outside of RL, e.g., semi-supervised learning [52], have also used lagging networks to stabilize training. More fully connecting ideas from these various approaches may prove fruitful in multiple areas of machine learning.

6 Discussion

Using functional regularization, we propose an alternative to target networks for stabilizing value estimation with bootstrapping and function approximation. Like target networks, we use a lagging set of parameters to stabilize estimation. However, critically, this is decoupled from target value estimation, instead taking the form of a functional prior. In this way, we can 1) use up-to-date target value estimates, thereby propagating reward information more quickly, and 2) separately control the degree of stabilization via the FR weight, κ . Indeed, by comparing the gradients resulting from TD losses with target networks and FR, we noted that target networks implicitly perform a form of FR, but with lagging target values and a non-independent weight ($\kappa = \gamma$). This helps illuminate why target networks stabilize training in practice, while also highlighting their drawbacks.

In benchmark domains with both discrete and continuous actions, we have demonstrated the benefits of FR Q -learning. First, by using a fixed policy to isolate value estimation from policy optimization, we demonstrated both faster value propagation and improved learning speed as compared with target networks. Then, we showed that using FR Q -learning during policy optimization consistently results

in improved sample efficiency and final performance across a range of diverse environments. Thus, FR provides a conceptually simple, easy to implement, and effective method for improving value estimation in deep RL.

While FR Q -learning requires an additional weighting parameter, κ , we noted that many values of $\kappa \in (0, 1]$ outperformed target networks across environments. We see κ as providing needed flexibility in setting the degree of regularization, unlike target networks, which cannot separately control this aspect. In our experiments, we used a fixed κ throughout training, however, future work could investigate methods for automatically adjusting κ during training [11] or conditioning it on individual state-action pairs. Likewise, other forms of FR losses, corresponding to alternative functional priors, may yield further improvement. Nevertheless, the FR Q -learning approach that we have presented here performs well across a wide range of environments, providing a drop-in replacement for target networks.

Acknowledgement

AP would like to thank Valentin Thomas, Julien Roy, and Voot Tangkaratt for valuable comments and discussions. GMM would like to thank Thomas Möllenhoff for providing feedback on the proof. AP is partially supported by the Open Philanthropy Project. MEK and GMM are partially supported by KAKENHI Grant-in-Aid for Scientific Research (B), Research Project Number 20H04247. CP thanks the Open Philanthropy Project, the NSERC Discovery grants program and the CIFAR AI Chairs program. AP also wants to thank Compute Canada and Calcul Quebec for the computational resources used in this work.

References

- [1] Richard S Sutton and Andrew G Barto. *Reinforcement learning: An introduction*. MIT press, 2018.
- [2] Hado Van Hasselt, Yotam Doron, Florian Strub, Matteo Hessel, Nicolas Sonnerat, and Joseph Modayil. Deep reinforcement learning and the deadly triad. *arXiv preprint arXiv:1812.02648*, 2018.
- [3] Volodymyr Mnih, Koray Kavukcuoglu, David Silver, Alex Graves, Ioannis Antonoglou, Daan Wierstra, and Martin Riedmiller. Playing atari with deep reinforcement learning. *arXiv preprint arXiv:1312.5602*, 2013.
- [4] Timothy P Lillicrap, Jonathan J Hunt, Alexander Pritzel, Nicolas Heess, Tom Erez, Yuval Tassa, David Silver, and Daan Wierstra. Continuous control with deep reinforcement learning. *arXiv preprint arXiv:1509.02971*, 2015.
- [5] Abbas Abdolmaleki, Jost Tobias Springenberg, Yuval Tassa, Remi Munos, Nicolas Heess, and Martin Riedmiller. Maximum a posteriori policy optimisation. *arXiv preprint arXiv:1806.06920*, 2018.
- [6] Tuomas Haarnoja, Aurick Zhou, Pieter Abbeel, and Sergey Levine. Soft actor-critic: Off-policy maximum entropy deep reinforcement learning with a stochastic actor. In *International Conference on Machine Learning*, pages 1861–1870. PMLR, 2018.
- [7] Scott Fujimoto, Herke Hoof, and David Meger. Addressing function approximation error in actor-critic methods. In *International Conference on Machine Learning*, pages 1587–1596. PMLR, 2018.
- [8] Matthew Hausknecht and Peter Stone. Deep recurrent q-learning for partially observable mdps. *arXiv preprint arXiv:1507.06527*, 2015.
- [9] Hado Van Hasselt, Arthur Guez, and David Silver. Deep reinforcement learning with double q-learning. In *Proceedings of the AAAI Conference on Artificial Intelligence*, volume 30, 2016.
- [10] Matteo Hessel, Joseph Modayil, Hado Van Hasselt, Tom Schaul, Georg Ostrovski, Will Dabney, Dan Horgan, Bilal Piot, Mohammad Azar, and David Silver. Rainbow: Combining improvements in deep reinforcement learning. In *Proceedings of the AAAI Conference on Artificial Intelligence*, volume 32, 2018.
- [11] Tuomas Haarnoja, Aurick Zhou, Kristian Hartikainen, George Tucker, Sehoon Ha, Jie Tan, Vikash Kumar, Henry Zhu, Abhishek Gupta, Pieter Abbeel, and Sergey Levine. Soft actor-critic algorithms and applications. *arXiv preprint arXiv:1812.05905*, 2018.

- [12] Ari S Benjamin, David Rolnick, and Konrad Kording. Measuring and regularizing networks in function space. *arXiv preprint arXiv:1805.08289*, 2018.
- [13] Ethan Knight and Osher Lerner. Natural gradient deep q-learning. *arXiv preprint arXiv:1803.07482*, 2018.
- [14] Joshua Achiam, Ethan Knight, and Pieter Abbeel. Towards characterizing divergence in deep q-learning. *arXiv preprint arXiv:1903.08894*, 2019.
- [15] Pingbo Pan, Siddharth Swaroop, Alexander Immer, Runa Eschenhagen, Richard E Turner, and Mohammad Emtiyaz Khan. Continual deep learning by functional regularisation of memorable past. *arXiv preprint arXiv:2004.14070*, 2020.
- [16] Marc G Bellemare, Yavar Naddaf, Joel Veness, and Michael Bowling. The arcade learning environment: An evaluation platform for general agents. *Journal of Artificial Intelligence Research*, 47:253–279, 2013.
- [17] Greg Brockman, Vicki Cheung, Ludwig Pettersson, Jonas Schneider, John Schulman, Jie Tang, and Wojciech Zaremba. Openai gym. *arXiv preprint arXiv:1606.01540*, 2016.
- [18] Matthias Plappert, Marcin Andrychowicz, Alex Ray, Bob McGrew, Bowen Baker, Glenn Powell, Jonas Schneider, Josh Tobin, Maciek Chociej, Peter Welinder, et al. Multi-goal reinforcement learning: Challenging robotics environments and request for research. *arXiv preprint arXiv:1802.09464*, 2018.
- [19] Christopher John Cornish Hellaby Watkins. Learning from delayed rewards. 1989.
- [20] Richard S Sutton. Learning to predict by the methods of temporal differences. *Machine learning*, 3(1):9–44, 1988.
- [21] Gerald Tesauro. Td-gammon, a self-teaching backgammon program, achieves master-level play. *Neural computation*, 6(2):215–219, 1994.
- [22] Brian Sallans and Geoffrey E Hinton. Reinforcement learning with factored states and actions. *The Journal of Machine Learning Research*, 5:1063–1088, 2004.
- [23] Martin Riedmiller. Neural fitted q iteration—first experiences with a data efficient neural reinforcement learning method. In *European Conference on Machine Learning*, pages 317–328. Springer, 2005.
- [24] Robert Goodell Brown. *Statistical forecasting for inventory control*. McGraw/Hill, 1959.
- [25] Charles C. Holt, Franco Modigliani, John F. Muth, and Herbert A. Simon. *Planning Production, Inventories, and Work Force*. Englewood Cliffs, 1960.
- [26] Everette S Gardner Jr. Exponential smoothing: The state of the art. *Journal of forecasting*, 4(1):1–28, 1985.
- [27] Nicolo Cesa-Bianchi and Gabor Lugosi. *Prediction, learning, and games*. Cambridge university press, 2006.
- [28] James Kirkpatrick, Razvan Pascanu, Neil Rabinowitz, Joel Veness, Guillaume Desjardins, Andrei A Rusu, Kieran Milan, John Quan, Tiago Ramalho, Agnieszka Grabska-Barwinska, et al. Overcoming catastrophic forgetting in neural networks. *Proceedings of the national academy of sciences*, 114(13):3521–3526, 2017.
- [29] Cuong V Nguyen, Yingzhen Li, Thang D Bui, and Richard E Turner. Variational continual learning. *arXiv preprint arXiv:1710.10628*, 2017.
- [30] Shirli Di-Castro Shashua and Shie Mannor. Trust region value optimization using kalman filtering. *arXiv preprint arXiv:1901.07860*, 2019.
- [31] Ian Osband, Charles Blundell, Alexander Pritzel, and Benjamin Van Roy. Deep exploration via bootstrapped dqn. In *Advances in neural information processing systems*, pages 4026–4034, 2016.
- [32] Ian Osband, Benjamin Van Roy, and Zheng Wen. Generalization and exploration via randomized value functions. In *International Conference on Machine Learning*, pages 2377–2386, 2016.
- [33] Steven Kapturowski, Georg Ostrovski, John Quan, Remi Munos, and Will Dabney. Recurrent experience replay in distributed reinforcement learning. In *International conference on learning representations*, 2018.

- [34] Emilio Parisotto, Francis Song, Jack Rae, Razvan Pascanu, Caglar Gulcehre, Siddhant Jayakumar, Max Jaderberg, Raphael Lopez Kaufman, Aidan Clark, Seb Noury, et al. Stabilizing transformers for reinforcement learning. In *International Conference on Machine Learning*, pages 7487–7498. PMLR, 2020.
- [35] Matthias Plappert, Rein Houthoofd, Prafulla Dhariwal, Szymon Sidor, Richard Y Chen, Xi Chen, Tamim Asfour, Pieter Abbeel, and Marcin Andrychowicz. Parameter space noise for exploration. In *International Conference on Learning Representations*, 2018.
- [36] Gavin A Rummery and Mahesan Niranjan. *On-line Q-learning using connectionist systems*, volume 37. University of Cambridge, Department of Engineering Cambridge, UK, 1994.
- [37] Emanuel Todorov, Tom Erez, and Yuval Tassa. Mujoco: A physics engine for model-based control. In *2012 IEEE/RSJ International Conference on Intelligent Robots and Systems*, pages 5026–5033. IEEE, 2012.
- [38] Marcin Andrychowicz, Filip Wolski, Alex Ray, Jonas Schneider, Rachel Fong, Peter Welinder, Bob McGrew, Josh Tobin, Pieter Abbeel, and Wojciech Zaremba. Hindsight experience replay. In *Advances in neural information processing systems*, pages 5055–5065, 2017.
- [39] Amir massoud Farahmand, Mohammad Ghavamzadeh, Csaba Szepesvári, and Shie Mannor. Regularized fitted q-iteration for planning in continuous-space markovian decision problems. In *2009 American Control Conference*, pages 725–730. IEEE, 2009.
- [40] John Schulman, Philipp Moritz, Sergey Levine, Michael Jordan, and Pieter Abbeel. High-dimensional continuous control using generalized advantage estimation. *arXiv preprint arXiv:1506.02438*, 2015.
- [41] Shirli Di-Castro Shashua and Shie Mannor. Kalman meets bellman: Improving policy evaluation through value tracking. *arXiv preprint arXiv:2002.07171*, 2020.
- [42] Zhongwen Xu, Joseph Modayil, Hado van Hasselt, Andre Barreto, David Silver, and Tom Schaul. Natural value approximators: Learning when to trust past estimates. In *Proceedings of the 31st International Conference on Neural Information Processing Systems*, pages 2117–2125, 2017.
- [43] Pierre Thodoroff, Audrey Durand, Joelle Pineau, and Doina Precup. Temporal regularization in markov decision process. *arXiv preprint arXiv:1811.00429*, 2018.
- [44] Pierre Thodoroff, Nishanth Anand, Lucas Caccia, Doina Precup, and Joelle Pineau. Recurrent value functions. *arXiv preprint arXiv:1905.09562*, 2019.
- [45] Jan Peters, Katharina Mulling, and Yasemin Altun. Relative entropy policy search. In *Proceedings of the AAAI Conference on Artificial Intelligence*, volume 24, 2010.
- [46] John Schulman, Sergey Levine, Pieter Abbeel, Michael Jordan, and Philipp Moritz. Trust region policy optimization. In *International conference on machine learning*, pages 1889–1897. PMLR, 2015.
- [47] John Schulman, Filip Wolski, Prafulla Dhariwal, Alec Radford, and Oleg Klimov. Proximal policy optimization algorithms. *arXiv preprint arXiv:1707.06347*, 2017.
- [48] Abbas Abdolmaleki, Jost Tobias Springenberg, Jonas Degraeve, Steven Bohez, Yuval Tassa, Dan Belov, Nicolas Heess, and Martin Riedmiller. Relative entropy regularized policy iteration. *arXiv preprint arXiv:1812.02256*, 2018.
- [49] Sham M Kakade. A natural policy gradient. *Advances in neural information processing systems*, 14, 2001.
- [50] Mohammad Emtiyaz E Khan, Alexander Immer, Ehsan Abedi, and Maciej Korzepa. Approximate inference turns deep networks into gaussian processes. In *Advances in neural information processing systems*, pages 3094–3104, 2019.
- [51] Siddhant Garg and Yingyu Liang. Functional regularization for representation learning: A unified theoretical perspective. *arXiv preprint arXiv:2008.02447*, 2020.
- [52] Kaiming He, Haoqi Fan, Yuxin Wu, Saining Xie, and Ross Girshick. Momentum contrast for unsupervised visual representation learning. In *Proceedings of the IEEE/CVF Conference on Computer Vision and Pattern Recognition*, pages 9729–9738, 2020.
- [53] John N Tsitsiklis. Asynchronous stochastic approximation and q-learning. *Machine learning*, 16(3):185–202, 1994.

- [54] Dimitri P Bertsekas and John N Tsitsiklis. *Neuro-dynamic programming*. Athena Scientific, 1996.

A Appendix

A.1 Code Snippet

DDPG and HER with Functional Regularization

```
def fr_ddpg_loss(self, rng, q_params, target_q_params,
                 actor_params, target_actor_params,
                 state, action, reward, next_state, done, goal):
    q_pred = jax.vmap(self.q_fun, (0, None, None, None))(q_params,
                                                         state,
                                                         goal,
                                                         action)

    - next_action = self.actor_fun(target_actor_params, next_state, goal)
    - next_q = jax.vmap(self.q_fun, (0, None, None, None))(target_q_params,
                                                         next_state,
                                                         goal,
                                                         next_action)

    + next_action = self.actor_fun(actor_params, next_state, goal)
    + next_q = jax.vmap(self.q_fun, (0, None, None, None))(q_params,
                                                         next_state,
                                                         goal,
                                                         next_action)

    next_value = jax.lax.stop_gradient(next_q[0])
    reward = jnp.reshape(reward, next_value.shape)
    done = jnp.reshape(done, next_value.shape)
    q_target = reward + 0.98 * (1 - done) * next_value
    q_target = jnp.clip(q_target, -50, 0)
    q_target = jnp.expand_dims(q_target, 0)
    assert len(q_pred.shape) == len(q_target.shape)
    q_loss = 0.5 * jnp.mean((q_pred - q_target) ** 2)
    + prior_q = jax.vmap(self.q_fun, (0, None, None, None))(target_q_params,
                                                         state,
                                                         goal,
                                                         action)
    + reg_loss = 0.5 * jnp.mean((q_prior - q_pred) ** 2)
    + q_loss = q_loss + self.reg_weight * reg_loss
    return q_loss
```

Figure 5: Code differences between DDPG + HER and FR DDPG + HER

DQN with Functional Regularization

```
def fr_dqn_loss(self, q_params, target_q_params, obs, action,
                reward, next_obs, done):
    q = self.q_fun(q_params, obs)
    q_action = jnp.take_along_axis(q, action, -1)

    - next_q = self.q_fun(target_q_params, next_obs)
    - next_q = self.q_fun(q_params, next_obs)
    next_value = jnp.max(next_q, -1, keepdims=True)
    assert reward.shape == next_value.shape
    target_q = reward + 0.99 * (1 - done) * next_value
    target_q = jax.lax.stop_gradient(target_q)
    assert q_action.shape == target_q.shape
    q_loss = 0.5 * jnp.mean((q_action - target_q) ** 2)
    + q_prior = self.q_fun(target_q_params, obs)
    + q_prior_action = jnp.take_along_axis(q_prior, action, -1)
    + reg_loss = 0.5 * jnp.mean((q_prior_action - q_action)**2)
    + q_loss = q_loss + self.reg_weight * reg_loss
    return q_loss
```

Figure 6: Code differences between DQN and FR DQN

A.2 Derivation

A.2.1 Q -learning with Target Network

Letting $R^{(t)} \equiv R(\mathbf{s}_t, \mathbf{a}_t)$, $Q^{(t)} \equiv Q(\mathbf{s}_t, \mathbf{a}_t)$ and $\Delta Q_{\bar{\theta}}^{(t)} \equiv \mathbb{E}[Q_{\bar{\theta}}^{(t+1)} - Q_{\bar{\theta}}^{(t)} | \mathbf{s}_t, \mathbf{a}_t] = \mathbb{E}[Q_{\bar{\theta}}^{(t+1)} | \mathbf{s}_t, \mathbf{a}_t] - Q_{\bar{\theta}}^{(t)}$

$$\begin{aligned}
\nabla_{\theta} l^{\text{target}}(\theta) &= -(R^{(t)} + \gamma \mathbb{E}_{P, \pi}[Q_{\bar{\theta}}^{(t+1)}] - Q_{\theta}^{(t)}) \nabla_{\theta} Q_{\theta}^{(t)} \\
&= -(R^{(t)} + \gamma(Q_{\bar{\theta}}^{(t)} + \Delta Q_{\bar{\theta}}^{(t)}) - Q_{\theta}^{(t)}) \nabla_{\theta} Q_{\theta}^{(t)} \\
&= -(R^{(t)} + \gamma(Q_{\bar{\theta}}^{(t)} + \Delta Q_{\bar{\theta}}^{(t)}) - (1 - \gamma + \gamma)Q_{\theta}^{(t)}) \nabla_{\theta} Q_{\theta}^{(t)} \\
&= -(R^{(t)} + \gamma Q_{\bar{\theta}}^{(t)} + \gamma \Delta Q_{\bar{\theta}}^{(t)} - (1 - \gamma)Q_{\theta}^{(t)} - \gamma Q_{\theta}^{(t)}) \nabla_{\theta} Q_{\theta}^{(t)} \\
&= -(R^{(t)} + \gamma \Delta Q_{\bar{\theta}}^{(t)} - (1 - \gamma)Q_{\theta}^{(t)}) \nabla_{\theta} Q_{\theta}^{(t)} + \gamma(Q_{\bar{\theta}}^{(t)} - Q_{\theta}^{(t)}) \nabla_{\theta} Q_{\theta}^{(t)} \\
&= -(R^{(t)} + \gamma \Delta Q_{\bar{\theta}}^{(t)} - Q_{\theta}^{(t)} + \gamma Q_{\theta}^{(t)}) \nabla_{\theta} Q_{\theta}^{(t)} + \gamma(Q_{\bar{\theta}}^{(t)} - Q_{\theta}^{(t)}) \nabla_{\theta} Q_{\theta}^{(t)} \\
&= -(R^{(t)} + \gamma(Q_{\theta}^{(t)} + \Delta Q_{\bar{\theta}}^{(t)}) - Q_{\theta}^{(t)}) \nabla_{\theta} Q_{\theta}^{(t)} + \gamma(Q_{\bar{\theta}}^{(t)} - Q_{\theta}^{(t)}) \nabla_{\theta} Q_{\theta}^{(t)}
\end{aligned}$$

A.2.2 Q -learning with Functional Regularization

$$\begin{aligned}
\nabla_{\theta} l^{\text{FR}}(\theta) &= -(R^{(t)} + \gamma \mathbb{E}_{P, \pi}[Q_{\bar{\theta}}^{(t+1)}] - Q_{\theta}^{(t)}) \nabla_{\theta} Q_{\theta}^{(t)} + \kappa(Q_{\bar{\theta}}^{(t)} - Q_{\theta}^{(t)}) \nabla_{\theta} Q_{\theta}^{(t)} \\
&= -(R^{(t)} + \gamma(Q_{\bar{\theta}}^{(t)} + \Delta Q_{\bar{\theta}}^{(t)}) - Q_{\theta}^{(t)}) \nabla_{\theta} Q_{\theta}^{(t)} + \kappa(Q_{\bar{\theta}}^{(t)} - Q_{\theta}^{(t)}) \nabla_{\theta} Q_{\theta}^{(t)}
\end{aligned}$$

A.3 Hyperparameters

A.3.1 Multi-Goal Environments

We based our implementation on <https://github.com/openai/baselines/tree/master/baselines/her>. Note that the batch size might look like it differs from [18], but is similar to what was actually used as discussed here: <https://github.com/openai/baselines/issues/314>.

Table 1: Multi-Goal Hyperparameters

Hyperparameter	Value
Policy Network Hidden Units	[256, 256, 256]
Q Network Hidden Units	[256, 256, 256]
Target Update Frequency	40
Target Update Rate τ	0.05
Batch Size	2^{12}
Optimizer	Adam
Learning Rate	$1\text{e-}3$
Exploration ϵ	0.1
Discount Rate γ	0.98

A.3.2 Atari Learning Environments

The architecture used can be found here: https://github.com/deepmind/dm-haiku/blob/7964d01f1c0dd907c8ea016ad1d1cc7ae48ac05d/examples/impala/haiku_nets.py

Table 2: Atari Hyperparameters

Hyperparameter	Value
Target Update Frequency	32000
Optimizer	Adam
Learning Rate	6.25e-5
Batch Size	32
Discount Rate γ	0.99
Exploration ϵ	1 \rightarrow 0.1 over 1M frames
Evaluation ϵ	0.05

A.4 Additional Results

A.4.1 Mujoco Control Suite

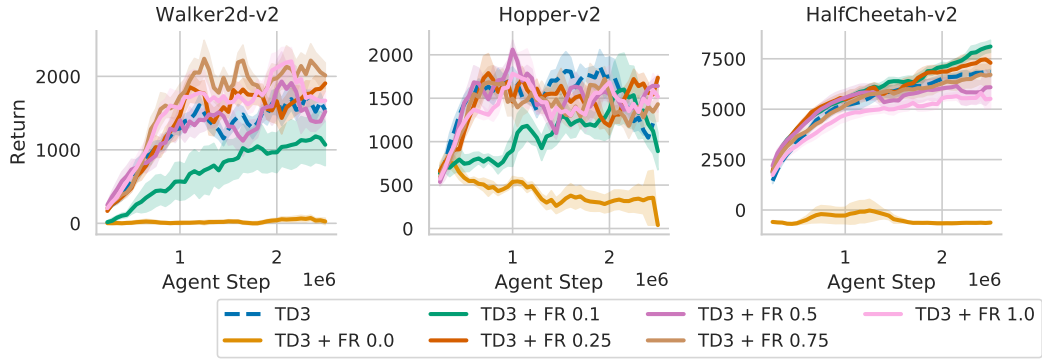


Figure 7: Performance curves for a subset of Mujoco tasks. FR does not provide substantial improvements as the reward is dense and the DNN architecture simple.

A.4.2 Atari CNN

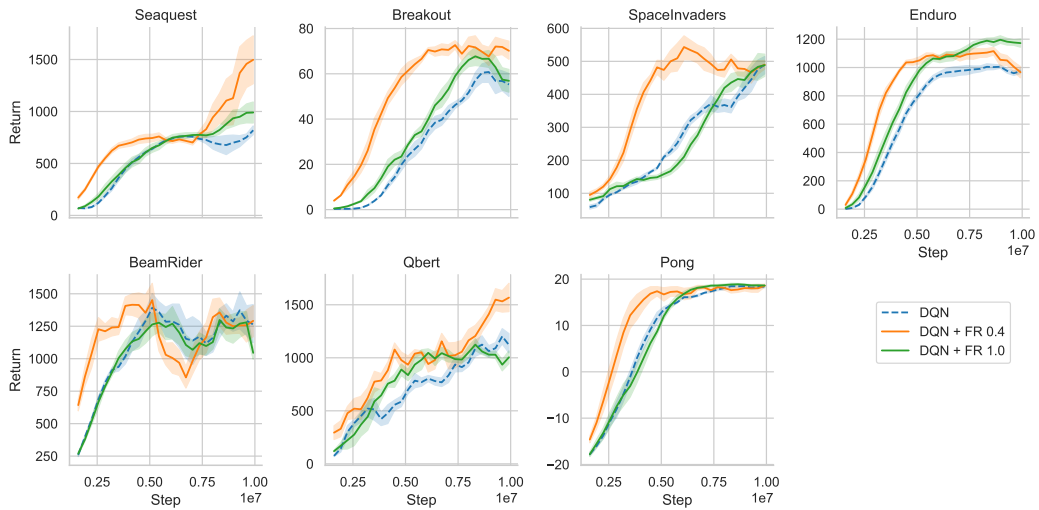


Figure 8: Performance curves for a subset of Atari games (same as [3]) for a CNN architecture. The baseline (dotted blue line) and two different FR weights (solid lines) average returns over 5 trials using a ϵ -greedy of 0.05 are reported.

A.5 Convergence of Q-learning with functional regularization in tabular setting

We want to prove that the Q-learning with functional regularization has convergence guarantees in the original setting where Q-learning was developed, *i.e.* the tabular scenario. Specifically, $Q: \mathcal{A} \times \mathcal{S} \rightarrow \mathbb{R}$ is a tabular function on the finite product space of states and actions. To prove our results, we start by proving a slight variation of a classical result from stochastic optimization [53]. Consider the algorithm defined by the iteration

$$\Delta_{i+1}(s) = (1 - \rho_t(\mathbf{s}_t, \mathbf{a}_t))\Delta_i(\mathbf{s}_t, \mathbf{a}_t) + \rho_t(\mathbf{s}_t, \mathbf{a}_t) \left[(T\Delta_i)(\mathbf{s}_t, \mathbf{a}_t) + u_i(\mathbf{s}_t, \mathbf{a}_t) + b_i(\mathbf{s}_t, \mathbf{a}_t) \right], \quad (9)$$

where $\mathcal{F}_i = \{(\Delta_0, \rho_0, \kappa_0, u_0), \dots, (\Delta_i, \rho_i, \kappa_i, u_i)\}$ and $\Delta_0(\mathbf{s}_t, \mathbf{a}_t) \in \mathbb{R}, \forall \mathbf{s}, \mathbf{a}$. We will show that this iteration generalizes the Q -function estimation error at iteration i for a generic state \mathbf{s}_t and generic action \mathbf{a}_t . First we make some assumptions.

1. $\rho_i(\mathbf{s}_t, \mathbf{a}_t) \in \mathbb{R}_+, \sum_{i=0}^{\infty} \rho_t(\mathbf{s}_t, \mathbf{a}_t) = \infty, \sum_{i=0}^{\infty} \rho_t^2(\mathbf{s}_t, \mathbf{a}_t) < \infty, \quad \forall \mathbf{s}, \mathbf{a}$
2. u_i is unbiased, *i.e.* $\mathbb{E}[u_i(\mathbf{s}_t, \mathbf{a}_t) | \mathcal{F}_i] = 0$
3. u_i has bounded variance, *i.e.* $\exists K_1 \in \mathbb{R}_+ : \mathbb{E}[u_i^2(\mathbf{s}_t, \mathbf{a}_t) | \mathcal{F}_i] \leq K_1 \|\Delta_i\|^2$
4. $T: \mathbb{R} \rightarrow \mathbb{R}$ is a contraction, *i.e.* $\|T\Delta_1 - T\Delta_2\| \leq \alpha \|\Delta_1 - \Delta_2\|$ for some $\alpha \in (0, 1)$ and some norm $\|\cdot\|$
5. Each state s is visited infinitely often with probability 1
6. Vanishing bias b_t , *i.e.* $\exists \kappa_i(\mathbf{s}_t, \mathbf{a}_t) \rightarrow 0 : |b_i(\mathbf{s}_t, \mathbf{a}_t)| \leq \kappa_i(\mathbf{s}_t, \mathbf{a}_t)(\|\Delta_i(\mathbf{s}_t, \mathbf{a}_t)\|_{\infty} + 1)$

We are ready to state a theorem and a lemma that we will use to prove convergence of the Q-learning iteration.

Lemma 1. *Given assumption 1 – 5, plus the assumption that $|b_i(\mathbf{s}_t, \mathbf{a}_t)| \leq 2C\|\Delta_t(s)\|_{\infty}$ for some $C > 1$, then $\|\Delta_t\|_{\infty}$ is bounded with probability 1.*

Proof. The proof of this lemma follows the structure the proof of proposition 4.7 in [54], however we leverage the fact that $b_i(\mathbf{s}_t, \mathbf{a}_t)$ is bounded by a value proportional to the current Δ_i (ass. 7) to allow for the algorithm to converge. All norms are maximum norms. We omit the arguments \mathbf{s}_t and \mathbf{a}_t for brevity. The whole proof hinges on enclosing Δ_0 in a hypercube of the form $\{\Delta : \|\Delta\| \leq G\}$ where G is chosen large enough so that $\|T\Delta_i\| \leq G$ whenever $\Delta_i \leq G$. In the absence of b_i this would imply that Δ_t stays inside such cube indefinitely. However, in the presence of noise Δ_i might exit the hypercube so that $\|\Delta_i\| > (1 + \epsilon)G$ for some $\epsilon > 0$, when that happens we reset G so as to enclose the latest value of Δ_i . Using the assumptions on the noise, we show that this reset on G , takes place only a finite number of times. For the sake of brevity we do not report the full proof here but instead highlight the differences with respect to the original proof.

The key difference is based on defining an auxiliary process $G'_i = 2CG_i$ for some $C \geq 1$ such that C is the minimum number verifying the inequalities $(\beta\epsilon - \eta)/C \leq 1$ and $(1 + \epsilon)/C \leq 1$. This process bounds G_i for all values of i . Indeed we have

$$\|\Delta_i\| \leq (1 + \epsilon)G'_i \quad \forall i \geq 0 \quad (10)$$

and

$$\|\Delta_i\| \leq G'_i, \quad \text{if } G'_{i-1} < G'_i. \quad (11)$$

Furthermore, for some D we have that $\|T\Delta_i\| \leq \beta\|\Delta_i\| + D \leq (\beta\epsilon + \eta)G_i \leq (\beta\epsilon + \eta)\frac{G'_i}{2C} \leq \frac{G'_i}{2}$. On the other hand, because $\|\Delta_i\| \leq (1 + \epsilon)G_i$, we can bound the bias with $b_i \leq 2\|\Delta_i\| \leq 2(1 + \epsilon)G_i \leq \frac{G'_i}{2C} \leq \frac{G'_i}{2}$. Hence we have the bound

$$\|T\Delta_i\| + b_i \leq G'_i. \quad (12)$$

We define the process $w'_i = u_i/G'_i$ that still satisfies assumption 2 and 3, and the process

$$W'_{i+1;i_0} = (1 - \rho_i)W'_{i;i_0} + \rho_i w'_i, \quad (13)$$

which is always smaller than ϵ for some $i \geq i_0$. Because G'_i bounds G_t , assumption 4.3 in [54] is verified for G'_i , the induction step for lemma 4.3 can now be rewritten as follows. Suppose there

exists some i_0 such that $\|\Delta_{i_0}\| \leq G'_{i_0}$ and such that eq. (4.30) and (4.31) of [54] hold. Then, for every $i \geq i_0$, we have $G'_i = G'_{i_0}$. Furthermore, for every $s \in \mathcal{S}$, we have

$$\begin{aligned} -G'_{i_0}(1 + \epsilon) &\leq -G'_{i_0} + W'_{i_0} G'_i \leq \Delta_i \\ &\leq G'_{i_0} + W'_{i_0} G'_{i_0} \leq G'_{i_0}(1 + \epsilon). \end{aligned}$$

The proof of this inequalities follows the proof of lemma 4.3 in [54], using Eq. (12). Therefore the process defined by Eq. (9) is always bounded with probability 1. \square

Theorem 2. *Given assumption 1 – 6, for each state, $\Delta_i(\mathbf{s}_t, \mathbf{a}_t)$ converges to 0.*

Proof. The proof of this theorem is the same as the proof of proposition 4.8 in [54]. \square

Theorem 3. *Consider the iteration*

$$Q_{i+1}(\mathbf{s}_t, \mathbf{a}_t) = Q_i(\mathbf{s}_t, \mathbf{a}_t) + \rho_i(\mathbf{s}_t, \mathbf{a}_t) \{ R(\mathbf{s}_t, \mathbf{a}_t) + \gamma \tilde{Q}_i - Q_i(\mathbf{s}_t, \mathbf{a}_t) \} + \quad (14)$$

$$+ \kappa_i(\mathbf{s}_t, \mathbf{a}_t) (Q_i(\mathbf{s}_t, \mathbf{a}_t) - \bar{Q}_i(\mathbf{s}_t, \mathbf{a}_t)) \quad (15)$$

with a sequence of steps $\rho_i(\mathbf{s}_t, \mathbf{a}_t)$ that satisfies assumption 1 and a sequence $\kappa_i(\mathbf{s}_t, \mathbf{a}_t)$ such that $\lim_{t \rightarrow \infty} \kappa_i(\mathbf{s}_t, \mathbf{a}_t) / \rho_i(\mathbf{s}_t, \mathbf{a}_t) \rightarrow 0$, $\kappa_i(\mathbf{s}_t, \mathbf{a}_t) \leq 1/2 \quad \forall \mathbf{s}, \mathbf{a}, i$ and every state is visited infinitely many times with probability 1. Then, this iteration converges to the minimum of Eq. (3).

Proof. We now proceed to show that Eq. (9) generalizes the Q-learning update in Eq. (14). Let us define $\tilde{Q}_i(s, a)$ to be a sample of expected Q-function $\mathbb{E}_P[Q(s, a)]$, then we can consider an iteration of SGD applied to Eq. (5):

$$\begin{aligned} Q_{i+1}(\mathbf{s}_t, \mathbf{a}_t) &= Q_i(\mathbf{s}_t, \mathbf{a}_t) + \rho_i(\mathbf{s}_t, \mathbf{a}_t) \left\{ R(\mathbf{s}_t, \mathbf{a}_t) + \gamma \tilde{Q}_i - Q_i(\mathbf{s}_t, \mathbf{a}_t) \right\} + \kappa_i(\mathbf{s}_t, \mathbf{a}_t) (Q_i(\mathbf{s}_t, \mathbf{a}_t) - \bar{Q}) \\ Q_{i+1}(\mathbf{s}_t, \mathbf{a}_t) &= (1 - \rho_t(s)) Q_i(\mathbf{s}_t, \mathbf{a}_t) + \kappa_i(\mathbf{s}_t, \mathbf{a}_t) (Q_i(\mathbf{s}_t, \mathbf{a}_t) - \bar{Q}) + \rho_i(\mathbf{s}_t, \mathbf{a}_t) \left\{ R(\mathbf{s}_t, \mathbf{a}_t) + \gamma \tilde{Q}_i \right\} \\ Q_{i+1}(\mathbf{s}_t, \mathbf{a}_t) &= (1 - \rho_i(s)) Q_i(\mathbf{s}_t, \mathbf{a}_t) + \kappa_i(\mathbf{s}_t, \mathbf{a}_t) (Q_i(\mathbf{s}_t, \mathbf{a}_t) - \bar{Q}) + \\ &\quad + \rho_i(\mathbf{s}_t, \mathbf{a}_t) \left\{ R(\mathbf{s}_t, \mathbf{a}_t) + \gamma \tilde{Q}_i(\mathbf{s}_{t+1}, \mathbf{a}_{t+1}) + \gamma \mathbb{E}[Q_i(\mathbf{s}_{t+1}, \mathbf{a}_{t+1})] - \gamma \mathbb{E}[Q_i(\mathbf{s}_{t+1}, \mathbf{a}_{t+1})] \right\}. \end{aligned}$$

we can now define: $\Delta_i := Q_i(\mathbf{s}_t, \mathbf{a}_t) - Q^*(\mathbf{s}_t, \mathbf{a}_t)$, where $Q^* : \mathcal{A} \times \mathcal{S} \rightarrow \mathbb{R}$ is the optimal Q-function minimizing Eq. (3). We assume Q^* to be 0 everywhere without any loss of generality. T is the Bellman operator; $u_i := \gamma \tilde{Q} - \gamma \mathbb{E}[Q_i(\mathbf{s}_{t+1}, \mathbf{a}_{t+1})]$; $b_i := \kappa_i(\mathbf{s}_t, \mathbf{a}_t) (Q_i(\mathbf{s}_t, \mathbf{a}_t) - \bar{Q})$. Because we do not have access to the transition dynamics P of the environment, SGD uses a sampled version of the expected value of Q_i , however introducing the unbiased noise u_i we can recover the true Bellman operator and still ensure convergence. Hence we have:

$$\begin{aligned} \underbrace{Q_{i+1}(\mathbf{s}_t, \mathbf{a}_t)}_{\Delta_{t+1}} &= (1 - \rho(\mathbf{s}_t, \mathbf{a}_t)) \underbrace{Q_i(\mathbf{s}_t, \mathbf{a}_t)}_{\Delta_t} + \\ &\quad + \rho_i(s) \left\{ \underbrace{R(\mathbf{s}_t, \mathbf{a}_t) + \gamma \mathbb{E}[Q_i(\mathbf{s}_{t+1}, \mathbf{a}_{t+1})]}_{(T\Delta_i)(\mathbf{s}_t, \mathbf{a}_t)} + \underbrace{\gamma \tilde{Q}_i - \gamma \mathbb{E}[Q_i(\mathbf{s}_{t+1}, \mathbf{a}_{t+1})]}_{u_t} + \right. \\ &\quad \left. + \underbrace{\frac{\kappa_i(\mathbf{s}_t, \mathbf{a}_t)}{\rho_i(\mathbf{s}_t, \mathbf{a}_t)} (Q_i(\mathbf{s}_t, \mathbf{a}_t) - \bar{Q})}_{b_i} \right\}. \end{aligned}$$

We now need to prove that assumptions 2, 3, 4, 6 hold.

Assumption 2. It's immediate to see that u_t has zero mean because \tilde{Q}_i is a sampled from $Q_i(\mathbf{s}_{t+1}, \mathbf{a}_{t+1})$, therefore $\mathbb{E}[\tilde{Q}_i(\mathbf{s}_{t+1}, \mathbf{a}_{t+1})] = \mathbb{E}[Q_i(\mathbf{s}_{t+1}, \mathbf{a}_{t+1})]$.

Assumption 3. $\mathbb{E}[u_i^2(\mathbf{s}_{t+1}, \mathbf{a}_{t+1}) | \mathcal{F}_i] \leq \gamma \max_{\mathbf{a} \in \mathcal{A}} \mathbb{E}[\tilde{Q}_i^2] + \gamma \max_{\mathbf{a} \in \mathcal{A}} \mathbb{E}[Q_i(\mathbf{s}_{t+1}, \mathbf{a})]^2 \leq \gamma K_1 \|\Delta_t\|^2$, for some positive K_1 .

Assumption 4. This is a classical result for the Bellman operator, we refer the reader to the proof of proposition 5.5 in [54].

Assumption 6. We can write the bias term as $b_i = \frac{\kappa_i(\mathbf{s}_t, \mathbf{a}_t)}{\rho_i(\mathbf{s}_{t+1}, \mathbf{a}_{t+1})}(\Delta_i - \Delta_{i-I})$ for some integer I . Because $(\Delta_i - \Delta_{i-I}) \leq 2\|\Delta\|_i$ and $\kappa_i(\mathbf{s}_t, \mathbf{a}_t) \leq 1/2 \forall \mathbf{s}, \mathbf{a}, i$, we have $b_i = \frac{\kappa_i(\mathbf{s}_t, \mathbf{a}_t)}{\rho_i(\mathbf{s}_t, \mathbf{a}_t)}(\Delta_i - \Delta_{i-I}) \leq \frac{\kappa_i(\mathbf{s}_t, \mathbf{a}_t)}{\rho_i(\mathbf{s}_t, \mathbf{a}_t)}(2\|\Delta_i(\mathbf{s}_t, \mathbf{a}_t)\| + 2) \leq \frac{\kappa_i(\mathbf{s}_t, \mathbf{a}_t)}{\rho_i(\mathbf{s}_t, \mathbf{a}_t)}(\|\Delta_i(\mathbf{s}_t, \mathbf{a}_t)\| + 1)$.

Since all assumptions are met, Eq. (14) converges to the optimal Q -function. \square